PAPER

The magnetic structures of GdCuSn, GdAgSn and GdAuSn

To cite this article: D H Ryan *et al* 2017 *J. Phys.: Condens. Matter* **29** 495804

View the article online for updates and enhancements.

The magnetic structures of GdCuSn, GdAgSn and GdAuSn

D H Ryan[1] , **J M Cadogan**[2] , **V I Krylov**[3], **Anaëlle Legros**[1], **Rasa Rejali**[1] **and C D Boyer**[4]

[1] Physics Department and Centre for the Physics of Materials, McGill University, 3600 University Street, Montreal, Quebec, H3A 2T8, Canada
[2] School of Physical, Environmental and Mathematical Sciences, UNSW Canberra at the Australian Defence Force Academy, Canberra, BC2610, ACT, Australia
[3] Moscow MV Lomonosov State Univ, Skobeltsyn Institute of Nuclear Physics, Moscow 119992, Russia
[4] Canadian Neutron Beam Centre, Chalk River Laboratories, Chalk River, Ontario K0J 1J0, Canada

E-mail: dhryan@physics.mcgill.ca

Abstract
We have determined the magnetic structures of GdCuSn, GdAgSn and GdAuSn using a combination of ^{155}Gd Mössbauer spectroscopy and neutron powder diffraction. Each compound shows the same antiferromagnetic ordering of the Gd sublattice. The magnetic cell is doubled along the crystallographic a-axis (propagation vector $\mathbf{k} = [\frac{1}{2}, 0, 0]$) with the moments aligned along the hexagonal c-axis, forming alternating ferromagnetic sheets of up/down Gd moments along the a-axis.

Keywords: magnetic structure, Mössbauer spectroscopy, neutron diffraction, antiferromagnet, gadolinium, intermetallic compound

(Some figures may appear in colour only in the online journal)

1. Introduction

The RTX (R = rare earth, T = 3d/4d/5d transition metal, X = p-block element) series forms a huge family of equiatomic (1:1:1) intermetallic compounds which adopt a variety of crystal and magnetic structures [1]. Within this larger group, the RTSn series (where T = Cu, Ag or Au) crystallise in either the hexagonal LiGaGe (space group P6$_3$mc #186) or the closely related disordered variant CaIn$_2$ structure (space group P6$_3$/mmc #194) (see the review by Gupta and Suresh and references therein [1]). In both structures, the R atoms occupy a single crystallographic site, the 2a, while the transition metal (T) and Sn atoms either occupy distinct 2b sites (the P6$_3$mc structure) or share a single 4f site (the P6$_3$/mmc structure). For T = Cu and Au, compounds with the light rare earths (La–Nd) form in the disordered P6$_3$/mmc structure [1–4] while those with the heavier rare earths (Gd–Ho) adopt the ordered P6$_3$mc structure [1, 5, 6]. For the silver series, the situation is less clear. Mazzone *et al* analysed their x-ray diffraction data in terms of the disordered P6$_3$/mmc structure for R = La–Yb (with the exception of Eu) [7], while a later neutron diffraction study by Baran *et al* found a slight preference for the ordered P6$_3$mc structure (R = Ce–Er, not Sm or Eu) [8]. The problem with the silver series comes from the extremely poor contrast between Ag and Sn in both x-ray and neutron diffraction measurements. For consistency, we have assumed the P6$_3$mc structure for all three GdTSn compounds studied here.

While the magnetic properties of the RTX series have been studied quite extensively (see the review by Gupta and Suresh and references therein [1]), most of the Gd-based compounds have been neglected due to perceived difficulties associated with carrying out neutron diffraction measurements with this highly absorbing element. Studies have therefore generally been restricted to simple bulk methods (e.g. susceptibility or magnetisation) or indirect local probes such as ^{119}Sn Mössbauer spectroscopy.

The magnetism of the GdTSn series was first studied by Oesterreicher [9] using ac-susceptibility measurements. The magnetisation curve at 5 K suggested purely antiferromagnetic (AF) ordering of the Gd sublattice, with $T_N^{Cu} = 24$ K and $T_N^{Au} = 35$ K. GdAgSn was reported to order AF at $T_N^{Ag} = 34$ K

[8, 10]. Bialic *et al* [11] used both ^{119}Sn and ^{155}Gd Mössbauer spectroscopy to show that the magnetic ordering temperature of GdCuSn was 28(2) K, broadly consistent with Oesterreicher [9], but found GdAuSn to be magnetically inhomogeneous and were unable to establish T_N^{Au}. More recent work places T_N^{Au} at 23 K [10] or 26 K [12]. While the primary transition temperatures are reasonably well established, there remains significant confusion about the magnetic structures of the GdTSn series. By combining information from the ^{119}Sn and ^{155}Gd Mössbauer data at 5 K Bialic *et al* [11] argued that the magnetic structure of GdCuSn consists of ferromagnetic (FM) chains of Gd moments parallel to the *c*-axis coupled AF in the *ab*-plane with a propagation vector $\mathbf{k} = [\frac{1}{2}, 0, 0]$. This structure is similar to those reported for TbCuSn, DyCuSn and HoCuSn [5]. However, multiple features in susceptibility or heat capacity data have led to claims of additional magnetic transitions in GdCuSn [5, 13], GdAgSn [10] and GdAuSn [10]. The presence/absence/size of these extra features vary inconsistently between reports, (for example, for GdCuSn three additional transitions at 3.5 K, 10 K and 13 K [5] or two at 6.6 K and 8.3 K [13]) suggesting that they may be due to the presence of varying amounts of otherwise undetected impurities. Reports of inhomogeneous Mössbauer spectra and multiple transitions have led to the suggestion that GdAgSn and GdAuSn may be spin glasses [10], despite the absence of both disorder and frustration (necessary, but not sufficient prerequisites for spin glass ordering) and the fact that many of the compounds with other rare earths exhibit long-ranged order (see Gupta and Suresh [1] and references therein).

In order to settle these issues, direct measurements of the magnetic structures of GdTSn (where T = Cu, Ag or Au) are essential. We present here a neutron powder diffraction study of all three compounds. We use a large-area flat plate sample mount [14] to reduce the impact of the large absorption cross section of natural gadolinium. The neutron diffraction work is complemented by ^{155}Gd Mössbauer spectroscopy. We find that all three compounds exhibit long-ranged AF magnetic order and adopt the same magnetic structure.

2. Experimental methods

The GdTSn, (T = Cu, Ag, Au) samples were prepared by arc-melting stoichiometric quantities of the pure elements (Gd 99.9 wt%, T 99.99 wt.% and Sn 99.999 wt%) under Ti-gettered argon. The resulting ingots were sealed under vacuum in quartz tubes and annealed for one week at 900 °C, followed by water quenching. Cu-K$_\alpha$ x-ray diffraction confirmed that the majority phase in the sample was the hexagonal GdTSn phase, with $\sim$2 wt.% of the corresponding $Gd_3T_4Sn_4$ compound present as an impurity. While several samples of each compound were prepared during this work, only the best exemplar of each compound (as determined by x-ray diffraction) was used for the studies presented here. This is a major advantage of using our large-area flat plate sample mount [14] rather than isotopically separated gadolinium. Pieces from a single 2 gram ingot could be used for all of the measurements (xrd, magnetometry, ^{155}Gd Mössbauer spectroscopy and neutron diffraction) so that they can be compared directly and with confidence.

Magnetic characterisation was carried out on a Quantum Design PPMS susceptometer/magnetometer equipped with a 9 T magnet and operated down to 1.8 K.

The ^{155}Gd Mössbauer spectra were obtained using a helium-flow cryostat to cool both the 50 mCi ^{155}SmPd$_3$ source and the sample. The drive was operated in sinusoidal mode and calibrated using a laser interferometer with velocities cross-checked against both ^{57}Co **Rh**/α-Fe at room temperature and ^{155}SmPd$_3$/GdFe$_2$ at 5 K. The spectra were fitted using a non-linear least-squares minimisation routine with line positions and intensities derived from an exact solution to the full Hamiltonian [15]. A transmission integral correction was applied in order to deal with the significant line overlap present in the spectra.

Neutron diffraction experiments were carried out on the C2 multi-wire powder diffractometer (DUALSPEC) at the NRU reactor, Canadian Neutron Beam Centre, Chalk River, Ontario. Temperatures down to 4 K were obtained using a closed-cycle refrigerator. The neutron wavelength was 1.327 22(17) Å. All refinements of the neutron diffraction patterns employed the FullProf/WinPlotr package [16, 17]. The scattering length is complex and is dominated by an imaginary term arising from Gd nuclear resonances. The scattering length is strongly dependent on the neutron energy and has been documented by Lynn and Seeger [18].

3. Results

3.1. Crystal structures

As noted above, the two proposed structures for the GdTSn compounds are closely related. One (P6$_3$mc, LiGaGe-type) is an ordered variant of the other (P6$_3$/mmc, CaIn$_2$-type), so distinguishing them depends on the scattering contrast between the T and Sn atoms. For T = Cu, Au this is relatively easy, but for T = Ag the very limited contrast in both neutron and x-ray scattering makes the problem challenging.

In figure 1 we show two fits to the room temperature (295 K) x-ray powder diffraction pattern of GdCuSn, obtained using CuK$_\alpha$ radiation. It is clear that the P6$_3$mc structure fits better than the P6$_3$/mmc structure does (the difference being most noticeable in the (101) peak at around $2\theta \sim 26°$). The refinement fit quality parameters for these two options are R(Bragg) = 12%, R(F) = 10%, Rwp = 9% and Rp = 9% for the P6$_3$mc structure and R(Bragg) = 14%, R(F) = 13%, Rwp = 11% and Rp = 10% for the P6$_3$/mmc structure. All further discussion throughout this paper will be in terms of the P6$_3$mc LiGeGa-type structure. In table 1 we give the crystallographic parameters derived from the Rietveld refinements of the x-ray diffraction data for all three compounds.

3.2. Ordering temperatures

The χ_{ac} data presented in figure 2 show evidence for an additional transition below the primary event in all three compounds. The feature in the GdAgSn trace is especially prominent, but even the GdAuSn shows some sign of an extra event [10]. We found the amplitude of the extra features to
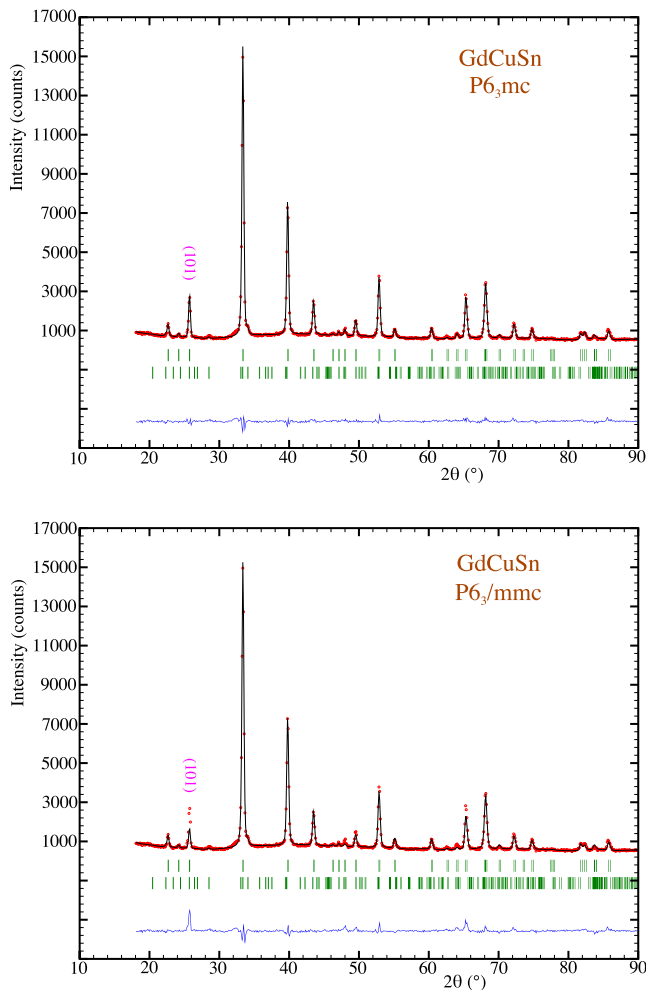
Figure 1. X-ray powder diffraction pattern of GdCuSn obtained at room temperature using CuK$_\alpha$ radiation. Top: refinement assuming P6$_3$mc structure; bottom: refinement assuming P6$_3$/mmc structure. Note the clear mis-fit of the (1 0 1) peak at around $2\theta \sim 26°$ in the P6$_3$/mmc refinement. The Bragg markers in each case are (top) primary GdCuSn (bottom) $\sim$2 wt.% Gd$_3$Cu$_4$Sn$_4$. The calculated residuals are shown at the bottom of each figure.

Table 1. Crystallographic data for GdTSn obtained by refinement of the 295 K XRD powder patterns, assuming the P6$_3$mc structure. Since the z parameters for all three sites are variable, we have fixed that of the Gd atom to be zero. This choice is equivalent to a translation of the entire cell along the *c*-axis and does not affect the final fit.

Atom	Site	x	y	z	T = Cu	T = Ag	T = Au
					z	z	z
Gd	2a	0	0	0*			
T	2b	$\frac{1}{3}$	$\frac{2}{3}$	z	0.810(7)	0.806(3)	0.814(2)
Sn	2b	$\frac{1}{3}$	$\frac{2}{3}$	z	0.228(6)	0.216(3)	0.223(2)

Note: z(Gd) = was fixed to 0.

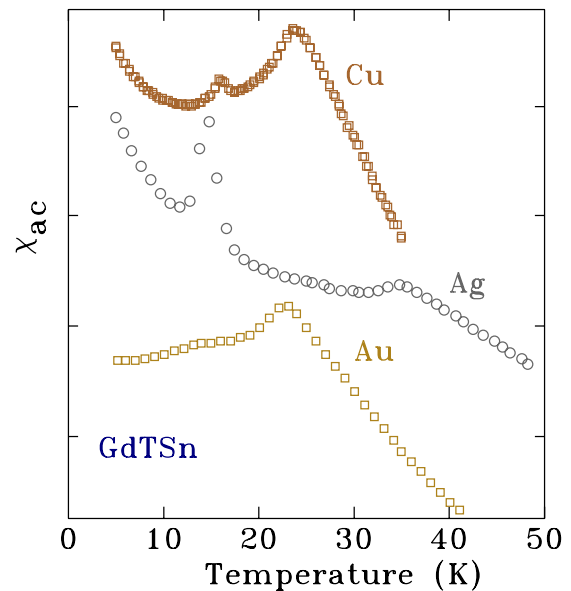|		
COPPER	a = 4.5331(4) Å	c = 7.3731(7) Å
SILVER	a = 4.7124(4) Å	c = 7.4326(8) Å
GOLD	a = 4.6570(3) Å	c = 7.4322(6) Å

Figure 2. Susceptibility data (χ_{ac}) for GdTSn taken at 1 kHz in a field of 1 mT. Secondary features are apparent in all three data sets.

be quite sample dependent and neither the ^{155}Gd Mössbauer spectra nor the neutron diffraction data showed any evidence for a change in magnetic ordering at the secondary χ_{ac} events (see below). Furthermore, while the $\sim$15 K events that we observe in GdAgSn and GdAuSn are broadly consistent with those previously reported by Łatka *et al* [10], the $\sim$16 K event for GdCuSn does not correspond to any of the five candidate features reported in earlier studies [5, 13]. We are therefore inclined to attribute the extra events to the presence of small, but highly responsive, impurities. While the Gd$_3$T$_4$Sn$_4$ impurities noted earlier in the x-ray diffraction data might appear to be potential candidates for the source of the extra features, they are, unfortunately, a very poor fit. Both Gd$_3$Cu$_4$Sn$_4$ and Gd$_3$Ag$_4$Sn$_4$ exhibit susceptibility features at $\sim$8 K, that are not associated with their primary ordering at 13 K (Cu) and 29 K (Ag) (the primary ordering does not yield a significant feature in the susceptibility [19]) and all of these events are far from the extra features: 16 K (Cu) and 15 K (Ag). We are not aware of any data on the Gd$_3$Au$_4$Sn$_4$ compound. The transition temperatures for the three compounds measured

using χ_{ac}, ^{155}Gd Mössbauer spectroscopy and neutron diffraction are summarised in table 2.

3.3. ^{155}Gd Mössbauer spectroscopy

The ^{155}Gd Mössbauer spectra of the three GdTSn compounds taken in the paramagnetic state are shown in figure 3 and at 5 K in figure 4. While the structures of the three compounds are the same, it is clear that the electric field gradient (*efg*) at the Gd site in GdAuSn is almost zero, very different from that in GdCuSn or GdAgSn as noted in previous work [11, 12]. Analysis of the 5 K spectra for GdCuSn and GdAgSn, where the *efg* is large, allows us to establish the sign of the *efg* (negative) and also to show that the Gd moments are parallel to the V$_{zz}$, the principal axis of the *efg* tensor. The point symmetry of the Gd(2a) site in the P6$_3$mc structure is 3*m*·, forcing the

Table 2. Transition temperatures for GdTSn taken from χ_{ac}, ^{155}Gd Mössbauer spectroscopy and neutron diffraction. The secondary events shown as second entries in the χ_{ac} column were only seen by χ_{ac}.

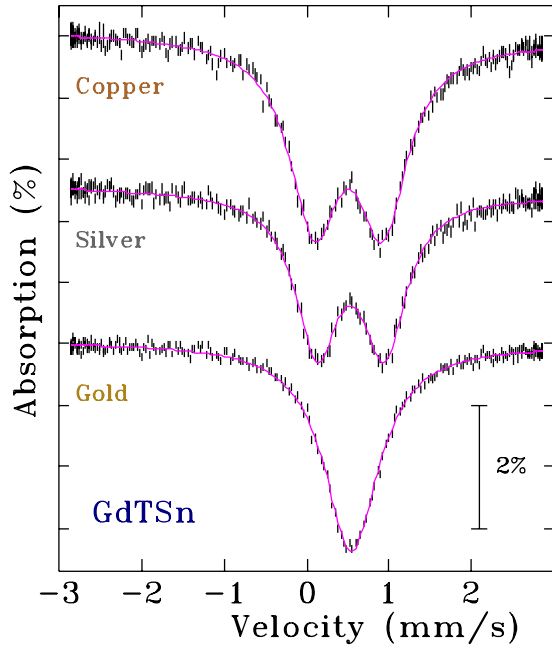|	χ_{ac}	Mössbauer	Neutron
GdCuSn	23.8 (2)	23.8 (1)	25.2 (2)
	16.0 (3)		
GdAgSn	34.8 (3)	34.5 (1)	37 (1)
	14.8 (3)		
GdAuSn	23.2 (3)	24.9 (2)	29.4 (4)
	14 (1)		

Figure 3. ^{155}Gd Mössbauer spectra of GdTSn taken in the paramagnetic state: Copper (25 K), Silver (40 K) and Gold (30 K). Note the absence of a quadrupole splitting for GdAuSn.

asymmetry parameter to be zero and placing V_{zz} parallel to the c-axis. Thus we conclude that the Gd moments in GdCuSn and GdAgSn (and most probably GdAuSn) are ordered parallel to the c-axis, as suggested by Bialic *et al* [11] for GdCuSn. No such analysis was possible in the case of GdAuSn as the observed quadrupole contribution was statistically consistent with zero, and for simplicity was set to zero in the analysis of the spectrum taken at 5 K. Our fitted hyperfine parameters for the ^{155}Gd Mössbauer spectra of the three GdTSn compounds are summarised in table 3.

In all three cases, no anomalies were seen in the temperature evolution of the spectral shape, and all of the ^{155}Gd Mössbauer spectra could be fitted assuming a single Gd component and a fixed ($\theta = 0$) orientation of B_{hf} with respect to V_{zz}. While we saw no evidence for the previously reported 'inhomogeneous' behaviour in GdAuSn [10, 11], we did observe an unusual temperature dependence in the hyperfine field, $B_{hf}(T)$. Figure 5 shows that while the $B_{hf}(T)$ for GdAuSn could be fitted using a simple $J = \frac{7}{2}$ Brillouin function, $B_{hf}(T)$ showed a clear break in behaviour, dropping more rapidly to zero and yielding a lower transition temperature than would be
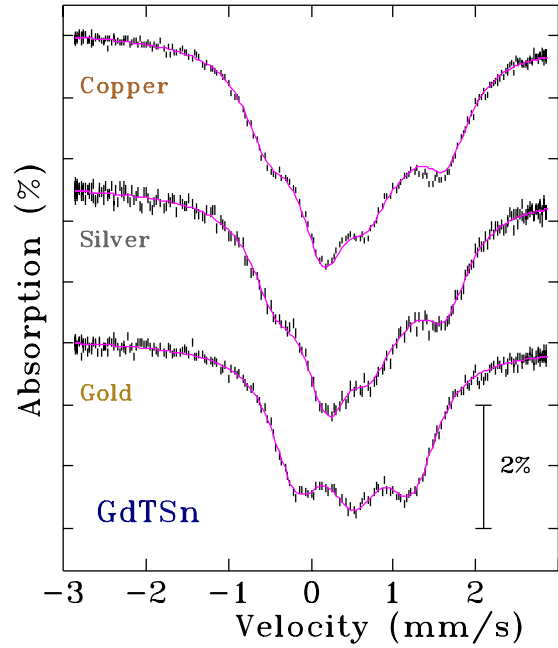

Figure 4. ^{155}Gd Mössbauer spectra of GdTSn taken at 5 K. All three compounds are clearly ordered with no apparent line broadening that might suggest non-collinear or spin-glass-like ordering.

Table 3. ^{155}Gd Mössbauer parameters for GdTSn. Quadrupole splitting (QS) from the paramagnetic state (see figure 3); Hyperfine field (B_{hf}) at 5 K; Angle (θ) between V_{zz} and B_{hf}. Since V_{zz} is necessarily parallel to the c-axis (see text for details) θ is also the angle between B_{hf} and the c-axis. Non-zero values for θ did not improve the fit for GdCuSn or GdAgSn so θ was fixed to zero for the final analysis. For the magnetic fits, QS was fixed to the value determined in the paramagnetic state, except for GdAuSn where it was fixed to zero so no value for θ could be fitted.

	QS (mm s^{-1})	B_{hf} (T)	θ
GdCuSn	$-1.74(1)$	24.4(2)	0
GdAgSn	$-1.73(3)$	23.7(2)	0
GdAuSn	$0.2(1)$	26.2(1)	—

expected from a direct extrapolation of the lower temperature behaviour (shown as dotted lines in figure 5). The break is less pronounced in GdAgSn and absent in GdAuSn. We emphasise that we observed no additional components in the ^{155}Gd Mössbauer spectra between the break and T_N, nor were there any changes in the quadrupole splitting that might indicate a change in moment direction or a structural transition. As the linewidths did not change, we can rule out dynamic effects, and the general agreement between Mössbauer-derived and neutron diffraction derived transition temperatures shown in table 2 is inconsistent with a break up to a short-range ordered state or some sort of spin-glass-like state.

3.4. Neutron powder diffraction

In figure 6 we show a comparison of the diffraction patterns obtained for GdCuSn at 40 K and 4 K, together with a difference plot. One immediate observation is that all of the high-angle peaks cancel perfectly, out to $2\theta = 58°$. (This actually
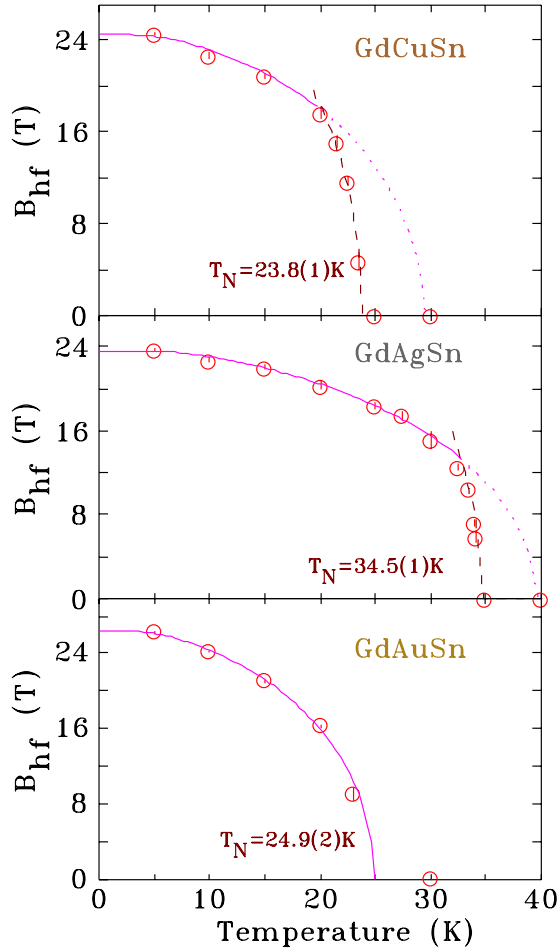
Figure 5. Temperature dependence of the [155]Gd hyperfine field in GdTSn showing the breaks in behaviour at $\sim$20 K in GdCuSn and $\sim$32 K in GdAgSn. The solid lines in each case are a fit to a $J = \frac{7}{2}$ Brillouin function with a dotted line showing the expected continuation for T = Cu and Ag.

Figure 6. Comparison of neutron diffraction patterns of GdCuSn obtained with a neutron wavelength of 1.327 22(17) Å. (top) Diffraction pattern taken at 40 K, well above T_N showing the nuclear-only scattering; (middle) pattern taken at 4 K, well below T_N showing the nuclear+magnetic scattering; (bottom) the difference between the 40 K and 4 K patterns showing the magnetic scattering.

that the gadolinium moments be static, while for a Bragg peak to be observed, long-ranged ordering must be present—the moments must be organised) it is instructive to compare the observed temperature dependences of the two signals. $B_{hf}(T)$ was shown earlier as figure 5, while the temperature dependence of the intensity of the ($\frac{1}{2}$ 0 0) peak is shown here in figure 7. The first observation is that the transition temperatures are consistent between the two techniques, with the neutron value being systematically higher in each case (table 2). This is inconsistent with dynamic or short-ranged ordering effects which would both lead to the reverse situation—moments can be static or quasi-static above the temperature at which they became organised, but the reverse is not possible. Remarkably, GdCuSn and GdAgSn exhibit the same anomalous temperature dependence in both signals. The peak intensity in GdCuSn could be fitted using a smooth curve ($J = \frac{1}{2}$ (squared) Brillouin function) with no break, while GdAgSn shows a clear break at essentially the same temperature in both signals. While it is likely that the 'break' reflects a limitation of the simple fitting form used, it is clear that in both GdCuSn and GdAgSn, the drop in ordered moment is both faster than would be expected, and the same whether the time-averaged (Mössbauer) or spatially-averaged (neutron) moment is measured. By contrast, GdAuSn follows the expected $J = \frac{7}{2}$ Brillouin function in both signals. These independent observations confirm that the unusual behaviour is real, and that it is associated with the long-ranged ordering of the gadolinium moments and not with the presence of magnetic inhomogeneity or spin-glass-like ordering.

3.4.1. The magnetic structure. As we found that the refinements of the neutron diffraction patterns for all three compounds, GdCuSn, GdAgSn and GdAuSn, yielded identical magnetic ordering modes, we will illustrate the magnetic

extends to the highest peaks seen, at $2\theta = 73°$). The cancellation was observed for all three compounds and allows us to rule out a change in lattice parameters at the $\sim$0.1% level, and makes it unlikely that the magnetic transition has any significant first-order character.

Three magnetic peaks in the 4 K pattern are quite clear in the difference plot, appearing at $2\theta \sim 10°$, $17°$ and $26°$. These Bragg positions are not allowed for nuclear (or ferromagnetic) scattering from the $P6_3mc$ space group, indicating that the magnetic structure at 4 K is antiferromagnetic. The purely magnetic peak at $2\theta \sim 10°$ indexes as ($\frac{1}{2}$ 0 0), indicating that the magnetic ordering of the Gd sublattice involves a cell-doubling in the hexagonal basal-plane, i.e. a propagation vector **k** = [$\frac{1}{2}$ 0 0]. All three compounds showed the same set of resolution-limited peaks at 4 K, indicating that they all adopted the same long-range ordered magnetic structure and allowing us to rule out disordered structures or spin-glass-like behaviour.

Given the related but complementary nature of [155]Gd Mössbauer spectroscopy and neutron diffraction (both provide a direct measure of the ordering of the gadolinium moments, but observation of a non-zero B_{hf} only requires
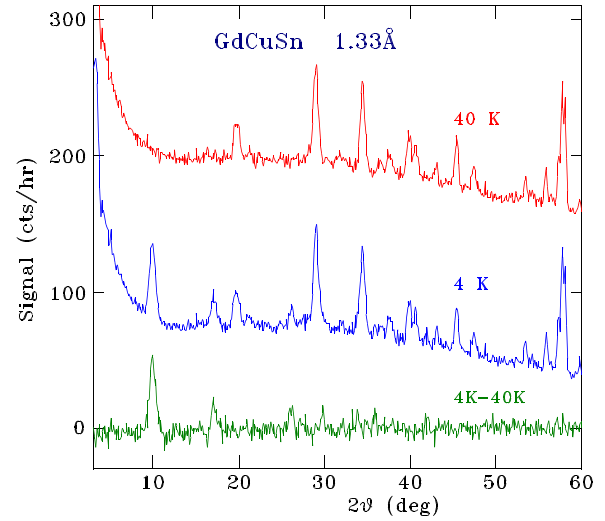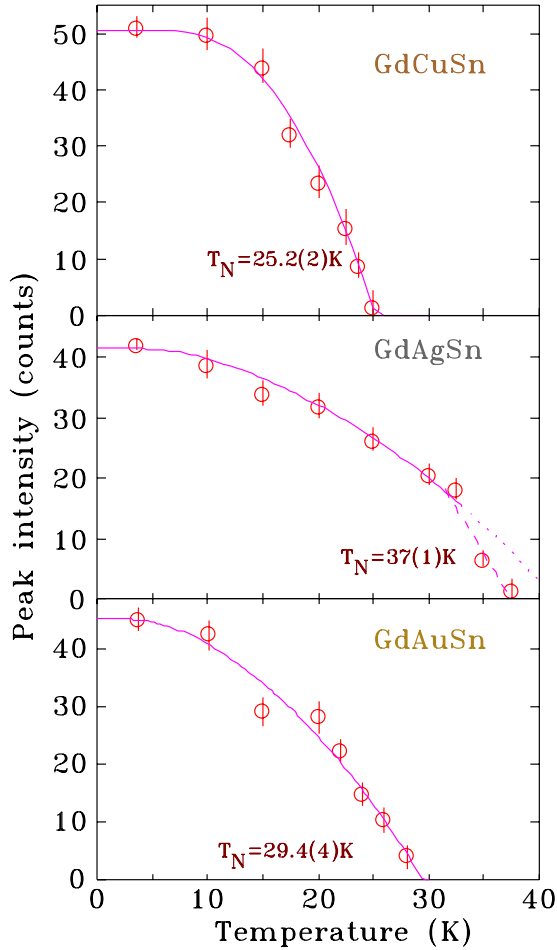
Figure 7. Temperature dependence of the $(\frac{1}{2}00)$ magnetic Bragg peak for (from top to bottom) GdCuSn, GdAgSn and GdAuSn. A clear evolution in behaviour is apparent. The data for GdAgSn and GdAuSn could be fitted using the expected $J = \frac{7}{2}$ (squared) Brillouin function, albeit with a break above 30 K for GdAgSn, while a $J = \frac{1}{2}$ (squared) Brillouin function was needed to fit the GdCuSn data.

structure determination process using only the GdCuSn data. At the end of this section, we will simply present the refinements and fitted parameters of GdAgSn and GdAuSn.

At 40 K, GdCuSn is paramagnetic and the neutron diffraction pattern is purely nuclear. We obtained the refinement to the crystal structure shown in the upper panel of figure 8. The crystallographic parameters are given in table 5. The fitted neutron diffraction pattern of GdCuSn obtained at 4 K, well below the Néel temperature, is shown in the lower panel of figure 8.

In order to determine the symmetry-allowed magnetic structures for the Gd site in the P6$_3$mc nuclear space group with $\mathbf{k} = [\frac{1}{2} \, 0 \, 0]$ we carried out representational analysis using the BASIREPS program [16]. The decomposition of the magnetic representation comprises four representations:

$$\Gamma^{2a}_{\mathrm{Mag}} = 1\Gamma_1 + 1\Gamma_2 + 2\Gamma_3 + 2\Gamma_4 \qquad (1)$$

using the notation employed in Basireps [16]. The basis vectors of these irreducible representations are given in table 4.

Thus, the symmetry-allowed ordering direction for the Gd magnetic moments with $\mathbf{k} = [\frac{1}{2} \, 0 \, 0]$ may involve components both along the hexagonal c-axis and in the hexagonal basal-plane. Two of the representations are purely planar. The best refinement to the 4 K diffraction pattern is with the Gd moments ordered along the crystal c-axis, corresponding to the Γ_3 representation. Our refinement showed that the planar magnetic component of the Γ_3 representation is zero, within error. This c-axis ordering of the Gd moments is fully consistent with the analysis of the ^{155}Gd Mössbauer shown in figure 4 and summarised in table 3, that showed that the hyperfine field (B$_{hf}$) was parallel to V$_{zz}$ (and hence the c-axis) for GdCuSn and GdAgSn.

The refined Gd magnetic moment for the Γ_3 axial order is $6.0(2)\mu_{\mathrm{B}}$. Results of the neutron powder diffraction analysis for all three compounds is given in table 5. The magnetic structure is illustrated in figure 9.

4. Discussion

Most of the RTSn compounds related to the three Gd-based ones studied here exhibit simple collinear AF order with a propagation vector $\mathbf{k} = [\frac{1}{2}, 0, 0]$ [3, 5, 6, 8]. With few exceptions, the rare earth moments are either parallel or perpendicular to the c-axis (e.g. the cerium moments in CeAgSn are canted by 40° from the c-axis [8]. Even where incommensurate order has been reported (e.g. in TbCuSn and HoCuSn [5], the simpler $\mathbf{k} = [\frac{1}{2}, 0, 0]$ structure is the first to form on cooling through T_N.

Given this broad consistency across the RTSn system, it would be rather surprising if the GdTSn set, with their relatively simple spherically-symmetric gadolinium ion, were outliers, exhibiting magnetic inhomogeneity [11] or spin-glass-like ordering [10]. It is probably no coincidence that these claims of unusual ordering were associated only with the gadolinium-based compounds, where the extreme neutron absorption cross-section generally renders them inaccessible to direct determination of their magnetic structures.

As we have shown here using a combination of ^{155}Gd Mössbauer spectroscopy and neutron powder diffraction, there is no evidence for inhomogeneity, slow dynamics or spin glass-like ordering in any of the GdTSn compounds studied here. The transition temperatures determined by χ_{ac}, ^{155}Gd Mössbauer spectroscopy and neutron diffraction (table 2) are all in agreement, and as they were determined using pieces taken from the same ingot, they are directly comparable. While multiple features were seen in the χ_{ac} data (figure 2) only the primary events at T_N were confirmed, and we attribute the extra (and highly variable) features to small, but highly responsive, impurities. This stands in clear contrast to the situation in, for example, CeAuSn and PrAuSn, where two transitions were seen by χ_{ac} and then confirmed by ^{119}Sn Mössbauer spectroscopy [4].

The magnetic structure that we have determined for all three GdTSn (T = Cu, Ag, Au) compounds studied here is a simple cell-doubled AF structure with the gadolinium
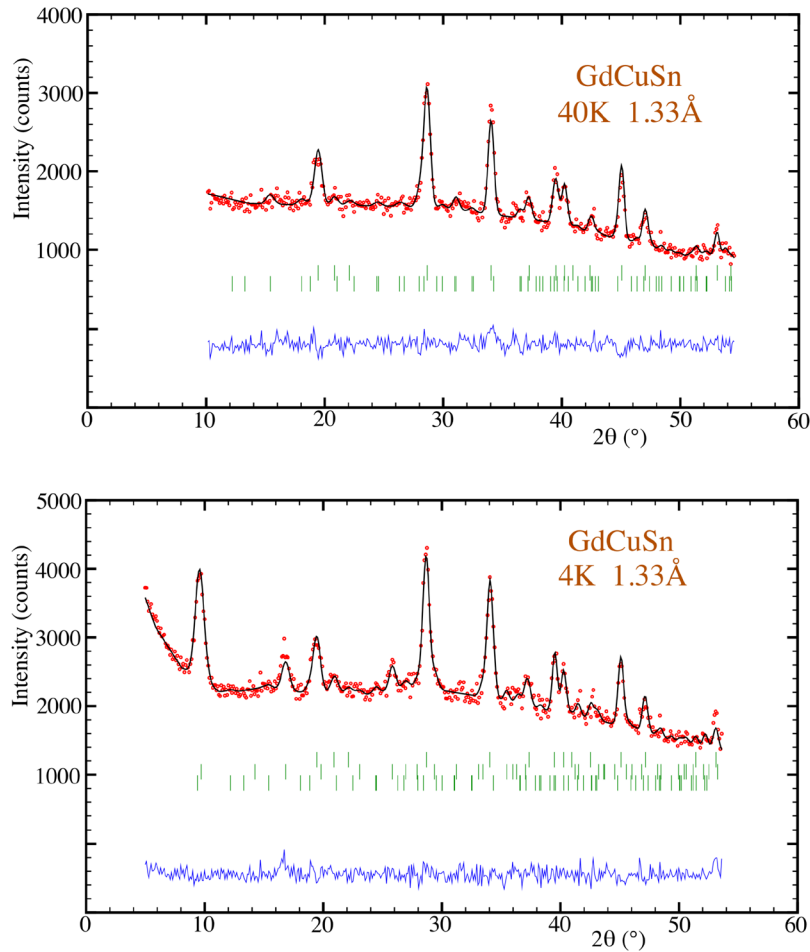
Figure 8. Refined neutron diffraction pattern of GdCuSn, obtained at (top) 40 K and (bottom) 4 K with a neutron wavelength of 1.327 22(17) Å. The Bragg markers are (from the top): primary GdCuSn, ~2 wt.% $Gd_3Cu_4Sn_4$, and magnetic scattering from the ordered GdCuSn (only in the 4 K pattern). The calculated residuals are shown at the bottom of each figure.

Table 4. Representation analysis for the Gd site in GdTSn with a propagation vector $[\frac{1}{2}\,0\,0]$.

Representation	Basis vector atom 1 $(0\,0\,0)$	Basis vector atom 2 $(0\,0\frac{1}{2})$
Γ_1	$[0\,u\,0]$	$[0\,-u\,0]$
Γ_2	$[0\,u\,0]$	$[0\,u\,0]$
Γ_3	$[2u\,u\,v]$	$[-2u\,-u\,v]$
Γ_4	$[2u\,u\,v]$	$[2u\,u\,-v]$

moments parallel to the *c*-axis and a propagation vector of $\mathbf{k} = [\frac{1}{2}, 0, 0]$ (see figure 9). This structure is found in many RTSn compounds. The magnetic Bragg peaks were observed to be resolution-limited, within error, at all temperatures where they were present, suggesting that a conventional long-range-ordered AF state forms on cooling through T_N. Furthermore, the agreement between the Mössbauer and neutron derived values for T_N allows us to rule out dynamic contributions to the ordering around T_N.

Finally, we observed an unusually rapid decline in the ordered gadolinium moment for two of the compounds studied here. In GdAuSn, both neutron diffraction and ^{155}Gd Mössbauer spectroscopy showed that the temperature dependence of the ordered moment could be fitted using the

Table 5. Crystallographic and magnetic data for GdTSn obtained by refinement of the 4 K neutron powder diffraction patterns taken at a wavelength of 1.327 22(17) Å. Since the z parameters for all three sites are variable, we have fixed that of the Gd atom to be zero. This choice is equivalent to a translation of the entire cell along the *c*-axis and does not affect the final fit. Note: only the component of the gadolinium moment parallel to the *c*-axis was found to be non-zero.

T	a (Å)	c (Å)	μ_c(Gd) (μ_B)
COPPER	4.531(6)	7.333(11)	6.0(2)
R(Bragg) = 12.8, R(F) 10.1, R(mag) = 14.4			
SILVER	4.708(4)	7.395(7)	7.2(2)
R(Bragg) = 7.3, R(F) 5.5, R(mag) = 17.1			
GOLD	4.648(3)	7.388(5)	5.6(2)
R(Bragg) = 11.2, R(F) 9.6, R(mag) = 19.5			

expected $J = \frac{7}{2}$ Brillouin function. The same function could fit the GdAgSn data up to ~0.85 T_N but a more rapid decline occurred above that point. For GdCuSn the effect was more severe and while the neutron data could be fitted satisfactorily using a steeper $J = \frac{1}{2}$ Brillouin function, this failed for the Mössbauer data and a break at ~0.85 T_N gave a better fit. We emphasise that we do not believe that these 'breaks' reflect a
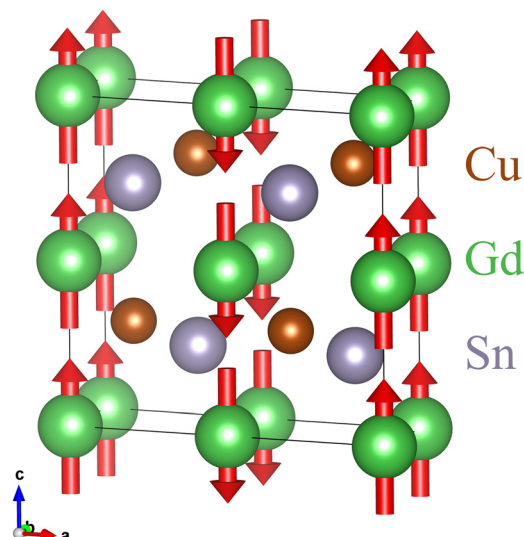
Figure 9. Magnetic structure of GdCuSn derived from analysis of our neutron diffraction data. The crystallographic cell is shown doubled along the *a*-axis. The gadolinium moments order parallel to the *c*-axis forming ferromagnetic sheets that are coupled antiferromagnetically along the *a*-axis. Figure drawn using the VESTA package [20].

real transition, as they are not associated with any changes in either the neutron diffraction or ^{155}Gd Mössbauer data, nor do they correspond to any of the extra features seen by χ_{ac}. Specifically, we saw no evidence for a coexistence region in the Mössbauer spectra (only a single magnetic or paramagentic component was needed to fit any given spectrum) nor did we find any evidence for a structural change in the neutron diffraction patterns. These observations would appear to rule out the possibility that the magnetic transition is first-order. It is more likely that the apparent breaks reflect a limitation of the fitting form used. It is clear, however, that the unusually rapid decline in ordered moment is a real feature of GdCuSn and GdAgSn, and this would bear further investigation.

5. Conclusions

We have determined the magnetic structures of GdTSn (T = Cu, Ag and Au) by using a combination of ^{155}Gd Mössbauer spectroscopy and neutron powder diffraction using our flat-plate technique for obtaining diffraction patterns from highly-absorbing samples [14]. The magnetic ordering temperatures of GdCuSn, GdAgSn and GdAuSn are 24(1) K, 35(1) K and 25(2) K, respectively. At 4 K, the magnetic order of the Gd(2a) sublattice in all three compounds is commensurate with the crystal lattice and involves a cell-doubling within the hexagonal basal-plane. The propagation vector is $\mathbf{k} = \left[\frac{1}{2}\, 0\, 0\right]$ and the Gd magnetic moments are aligned along the hexagonal *c*-axis. We find no evidence for the presence of magnetic inhomogeneity or spin-glass-like ordering.

ORCID iDs

D H Ryan ⓘ https://orcid.org/0000-0003-3858-1894
J M Cadogan ⓘ https://orcid.org/0000-0002-5414-0602
C D Boyer ⓘ https://orcid.org/0000-0003-1693-6033

References

[1] Gupta S and Suresh K 2015 *J. Alloys Compd.* **618** 562–606
[2] Sakurai J, Kegai K, Nishimura K, Ishikawa Y and Mori K 1993 *Physica* B **186–8** 583–5
[3] Baran S, Hofmann M, Leciejewicz J, Ślaski M and Szytuła A 1998 *J. Phys.: Condens. Matter* **10** 2107–14
[4] Łatka K, Chajec W, Kmieć R and Pacyna A W J 2001 *J. Magn. Magn. Mater.* **224** 241–8
[5] Baran S, Ivanov V, Leciejewicz J, Stüsser N, Szytuła A, Zygmunt A and Ding Y 1997 *J. Alloys Compd.* **257** 5–13
[6] Baran S, Leciejewicz J, Ślaski M, Hofmann P and Szytuła A 1998 *J. Alloys Compd.* **275–7** 541–4
[7] Mazzone D, Rossi D, Marazza R and Ferro R 1981 *J. Less-Common Met.* **80** P47–52
[8] Baran S, Leciejewicz J, Stüsser N, Szytuła A, Zygmunt A and Ding Y 1997 *J. Magn. Magn. Mater.* **170** 143–54
[9] Oesterreicher H 1977 *J. Less-Common Met.* **55** 131–3
[10] Łatka K, Görlich E A, Chajec W, Kmieć R and Pacyna A W J 1997 *J. Alloys Compd.* **262–3** 108–13
[11] Bialic D, Kruk R, Kmieć R and Tomala K 1997 *J. Alloys Compd.* **257** 49–56
[12] Casper F, Ksenofontov V, Kandpal H C, Reiman S, Shishido T, Takahashi M, Takeda M and Felser C 2006 *Z. Anorg. Allg. Chem.* **632** 1273–80
[13] Sebastian C P, Rayaprol S and Pöttgen R 2006 *Solid State Commun.* **140** 276–80
[14] Ryan D H and Cranswick L M D 2008 *J. Appl. Crystallogr.* **41** 198–205
[15] Voyer C J and Ryan D H 2006 *Hyperfine Interact.* **170** 91–104
[16] Rodríguez-Carvajal J 1993 *Physica* B **192** 55–69
[17] Roisnel T and Rodríguez-Carvajal J 2001 *Mater. Sci. Forum* **378-381** 118–23
[18] Lynn J E and Seeger P A 1990 *At. Data Nucl. Data Tables* **44** 191–207
[19] Voyer C J, Ryan D H, Napoletano M and Riani P 2007 *J. Phys.: Condens. Matter* **19** 156209
[20] Momma K and Izumi F 2011 *J. Appl. Crystallogr.* **44** 1272–6